Potential of Digital Color Imagery for Censusing Haleakala Silverswords in Hawaii

Rick E. Landenberger, James B. McGraw, Timothy A. Warner, and Tomas Brandtberg

Abstract

Spatially explicit, high spatial resolution remotely sensed imagery offers a largely untapped potential for censusing and monitoring rare plant populations that exist in remote, exposed environments. Using digital color imagery acquired over the Haleakala Crater on Maui, Hawai'i, we evaluated the accuracy of photointerpretation and automated censuses by imaging nine silversword census plots characterized by individuals of known size, life cycle status, and location. Due to spatial resolution limitations, both methods tended to omit small individuals, but omissions varied by size class and type of omission. Omission rates were low for demographically important medium and large plants; however, the automated method often failed to segment and census tightly clustered plants. The photointerpreter commission error rate was lower than that of the automated method, and both methods tended to overestimate mean silversword size. These data outline the issues and challenges that will likely emerge as spatially explicit, high spatial resolution aerial censuses become more common.

Introduction

Developing an effective management strategy for sustaining or restoring rare plant populations depends on accurate estimates of abundance over time (Gaston, 1994). Censusing methods range from presence/absence determinations to repeated censuses supplemented by data sufficient to parameterize a demographic model (Menges and Gordon, 1996). Demographic monitoring (Travis and Sutter, 1986), where individuals are followed over time, is the preferred method of monitoring when it is desirable to make projections of population fate and understand controls over population growth rate (Menges and Gordon, 1996; Caswell, 2001). Because sustaining rare plant populations depends on an understanding of the factors that influence population dynamics, demographic monitoring is a useful tool for both conservation biologists and natural resource managers.

Repeated censuses can be strengthened when coupled with spatial information about the population (Pavlik, 1994). High spatial resolution remote sensing is becoming more common (Coultier *et al.*, 2000; Peters *et al.*, 2000), and offers largely untapped potential for censusing, monitoring, and managing rare plant populations (McGraw *et al.*, 1998). First, in environments where access and terrain limit the intensity and extent of field-based census methods, remote sensing may be particularly valuable. Second, remote sensing makes it possible to census large areas and more individuals than is practical with ground-based methods. Third, in environments that are sensitive to human disturbance, remote sensing provides a low-impact data collection method. Fourth, the data contained in remote sensing imagery are spatially explicit and can be coregistered temporally, allowing not only assessment of individual fates over time, but also the association of survival, growth, reproduction, and mortality with physical and ecological features of the surrounding landscape.

In the present study, all of these potential advantages provided motivation to investigate the application of the remote-sensing approach to conservation of Hawaiian silverswords (genus *Argyroxiphium* [Asteraceae–Madiinae]). Endemic to the island of Maui, the Haleakala silversword (*Argyroxiphium sandwicense* subsp. *macrocephalum*) is a federally listed threatened species whose natural range is restricted to cinder cones and lava flows above 2,200 m within the crater of the Haleakala volcano. Probably numbering in the hundreds of thousands prior to European settlement, by 1920 the population was nearly extinct due to goat and cattle browsing, as well as collection by tourists who picked the plants to document their trip to the summit (Loope and Medeiros, 1994).

Ungulate removal, visitor education, law enforcement, and wilderness designation of much of the crater area has resulted in an extraordinary recovery of the Haleakala silversword, one of the most dramatic conservation success stories (Kobayashi, 1991; Loope and Medeiros, 1994). The most recent complete census estimated 48,400 individuals (Starr and Martz, unpublished data, 2001). However, the population has recently become vulnerable to a new and perhaps more insidious threat. A small, disjunct population of the exotic Argentine ant (*Linepithema humile*), one of the most invasive and destructive ant species in the world (Brian, 1983), was first documented near the summit of Haleakala in 1982 (Cole *et al.*, 1992), and has since spread to several other summit locations. Native pollinators, whose services are required by the self-incompatible silversword (Carr *et al.*, 1986), have been significantly reduced in areas where the ant is concentrated (Cole *et al.*, 1992). If ants spread throughout the crater, the effects on silversword seed set and recruitment could be devastating (Forsyth, unpublished data, 2001).

Our aerial census was designed to answer several important practical monitoring questions. How accurate is the silversword census using high-resolution digital color (RGB) imagery? In particular, we asked how accurately silverswords of various size could be censused by comparing information extracted from imagery with ground reference data from the 2000 field census. Image information was extracted both by human photointerpreters (Lloyd *et al.*, 2002) and by an algorithm developed specifically for this purpose. Second, we examined the ability to extract informa-

R.E. Landenberger and J.B. McGraw are with the Biology Department and T.A. Warner and T. Brandtberg are with the Geology and Geography Department, all at West Virginia University, Morgantown, WV 26506-6057 (rlanden@wvu.edu).

Photogrammetric Engineering & Remote Sensing
Vol. 69, No. 8, August 2003, pp. 915–923.

0099-1112/03/6908–915$3.00/0

tion from imagery on the size of silversword plants, including the distribution of sizes in the natural population. Both of these elements of a census are important for providing information needed to determine population trends. With repeated censuses, size, stage, and fate information could lead to demographic models and population viability analyses, both powerful tools for conservation of rare species (Brook *et al.*, 2000; Caswell, 2001).

Methods and Materials

Species

A. sandwicense plants are large, single-stemmed monocarpic rosettes, ranging in diameter from less than 5 cm to greater than 1 m (Figure 1).

Although silverswords can live longer than 60 years, their mean and maximum lifespans are unknown. Individuals remain compact rosettes until flowering, when an erect, 1.0- to 2.5-m central flowering stalk emerges, bearing 100 to 500 maroon flower heads. After producing seeds, the plant dies, leaving behind a dense grey mass of slowly decaying leaves and stem that can remain as long as ten years (Perez, 2001). Silverswords are the most prominent species on the floor of the Haleakala crater and on cinder cones; other plants are sparse and generally inconspicuous.

Ground Reference

Eleven annual census plots (5 m by 20 m) were established in 1985 by the Haleakala National Park Research Unit, Pacific Island Ecosystems Research Center. Plot locations were selected based on their representative silversword densities and geographical distribution across the Haleakala crater (Loope and Crivellone, 1986). Individual plots were divided into subplots (5 m by 5 m) using plastic stakes (Figure 2).

All eleven plots were located on cinder cones within the Haleakala Wilderness unit of the Park, at approximately N 20° 43′, W 156′ 13′. On 02 and 03 October 2000, diameter, location, and status (flowering, vegetative, dead) were recorded and mapped for all silverswords on each plot (Starr and Martz, unpublished data, 2000). Because dead silverswords are only recorded in the year of death (then no longer tracked), annual census maps dating from 1992 were also examined and used to identify old dead plants in the imagery. In order to relate ground reference data to aerial imagery, plot census maps were digitally scanned at 800 dots per inch and co-registered to the ADAR images using the Erdas Imagine 8.4 Geometric Correction module (Erdas, 1999). Data from the maps were then used to create a point vector layer and digitized over census plot imagery to create a series of spatially explicit, digital monitoring maps (Figure 3).

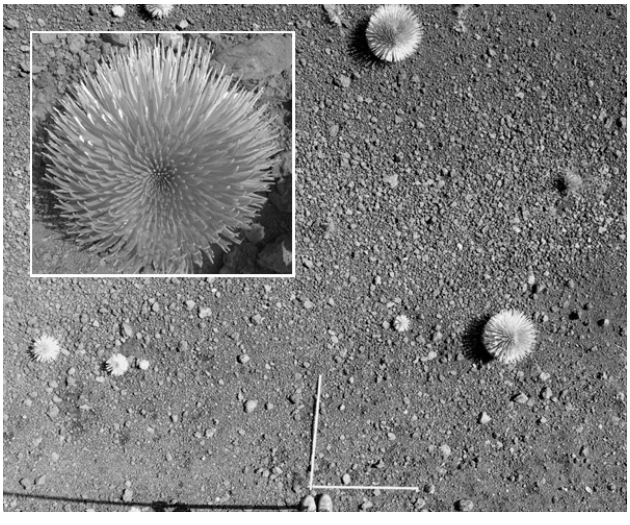

Figure 1. Vertical view of silverswords on an annual census plot taken from 5 m above ground level. The measuring sticks measure 1 m on a side. The silversword shown in the inset is 40 cm in diameter.

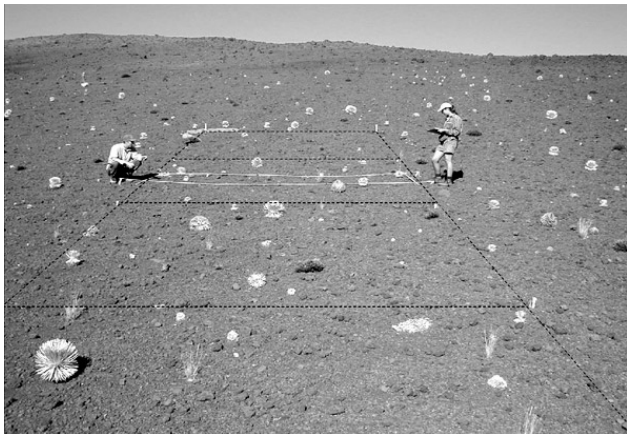

Figure 2. A 5- by 20-m annual census plot, with 5- by 5-m subplot boundaries delineated in the image.

Image Acquisition

Imagery was acquired using a Positive Systems ADAR 1000 imaging system (Positive Systems, 1999). The system consisted of a Kodak DCS 460C digital camera, associated housing, through-the-lens video targeting system, and differential GPS capability, all controlled by a laptop Pentium 133 computer running Windows NT 4.0. The camera was a Nikon N90s with a 20-mm focal length lens and a Kodak KAF 2300 CCD array (2048 by 3072, or 6.29 megapixels). Each pixel was 9 μm wide and coated with filters to produce a Bayer color array (Bayer, 1976). Every two-by-two array consisted of two pixels sensitive to green, one to red, and one to blue (or color-infrared). The lens transmitted light evenly across the visible range to the near infrared (400 to 800 nm) (Dean *et al.*, 2000). A combination ultraviolet near-infrared filter was employed to block the UV and near-infrared wavelengths. The decision to use color rather than color-infrared imagery was based on an initial investigation of the silversword population using field spectra and color 35-mm film. Preliminary findings indicated that photointerpreters could distinguish living from dead plants based on their respective differences in brightness. Furthermore, because only 25 percent of the pixels record near-infrared radiation when the camera is in color-infrared mode, any analysis of small silverswords has to be predominantly spatial rather than spectral.

The system was flown in a Bell 206B helicopter with a custom-built belly mount on 08 October 2000. Between 09:00 and 10:00 several transects were flown across the crater over the census plots. The camera exposure was set manually to *f* 2.8 with a shutter speed of 1/600 s. Nine of the 11 plots had been marked prior to the flight using blue flagging placed in an 'L' pattern at plot corners, and were referenced to GPS coordinates. Images were acquired at ap-

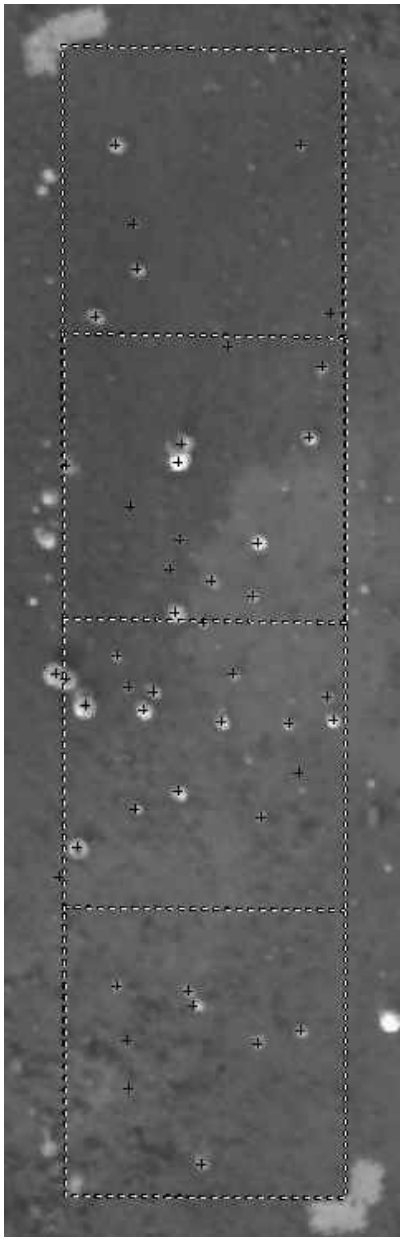

Figure 3. A grey-scale digital ADAR image taken from 100 m above ground level showing plot boundary polygons and individuals silversword point vector layers.

proximately 100 m above ground level directly above each plot. The ground sample distance (GSD) for each image pixel was 4 to 5 cm.

Automated Image Processing and Analysis

ADAR Image Interpolation

The interpolation of the raw images and subsequent image processing were carried out using custom programs written in Interactive Data Language (IDL) Version 5.4 (Research Systems, 1999). In the interpolation step, the raw ADAR Bayer color array was expanded to form a three-band (RGB) color image. Each pixel from the original image was assigned to the appropriate band–red (R), green (G), or blue (B)–depending on the wavelength sensitivity of the pixel location in the CCD. Thus, the digital numbers (DNs) are initially sparsely specified for each band. The interpolations of the red and blue bands were progressively carried out based on two sequential passes through the images. For the first pass, interpolation was limited to the locations where four diagonal neighbor pixels have specified values. The second scan interpolated the remaining pixel values, using both the original and previously interpolated values. The green band, on the other hand, has fewer empty pixels, and therefore required only a single interpolation.

Automated Detection of Silverswords

Silverswords are characterized as bright circular objects in the color ADAR images. Large individuals (≥20 cm diameter) show a silver-green hue, while smaller individuals are indistinctly grey. Therefore, only the intensity values from the transformation of the RGB data to intensity, hue, and saturation (Russ, 1998) were used in the image analysis. The intensity values were slightly Gaussian smoothed (σ = 1.0 pixels) to remove noise and other small artifacts from the interpolation. Smoothing is a process in which each pixel is replaced by the average of a local region of pixels. Gaussian smoothing is where the weighting of each pixel in calculating the local average declines with distance from the center position, following a Gaussian function.

The ADAR images, and the intensity bands in particular, suffer from a characteristic darkening at the image edge. For simplicity, this darkening is referred to as vignetting in this paper, although it results from a variety of causes including imaging geometry, lens properties, and internal shadowing in the camera. The first step in vignette correction was to apply a strong Gaussian smoothing (σ = 250.0 pixels) to the original intensity image. Second, to suppress the vignette effect, the image intensity value $I_{smoothed\ (\sigma=1)}$ is normalized by the smoothed intensity value $I_{smoothed\ (\sigma=250)}$, and the result is scaled by the maximum intensity (DN) in the image ($I_{global\ \max}$) i.e.,

$$I_{normalized} = \frac{I_{smoothed\ (\sigma=1)}}{I_{smoothed\ (\sigma=250)}} I_{global\ \max} \quad (1)$$

In the normalized intensity image, most silverswords can be distinguished as bright circular objects on a dark background (Figure 4A).

If the image grey levels (DNs) are thought of as height levels, and the image itself as a surface in three dimensions, the surface corresponding to a single silversword is a curved convex shape compared to the relatively flat background areas (Figure 4B). This contrast in surface shape was identified using the direction-independent measure of mean curvature, H (Gray, 1998; Wallace and Price, 2002) (Figure 4C). H is a geometric measure, and is calculated from partial derivatives of the slope of the surface (Rade and Westergren, 1995). The natural choice of a threshold level for an H-image is zero, because convex surfaces such as silverswords are associated with negative values (Figure 4D).

Silverswords are not the only convex surfaces in the image; indeed they are a minority of convex surfaces in the image. Bright rocks, other plants, and even random image tones can have a convex surface. However, silverswords have distinctively smooth and consistently curved surfaces that result in a comparatively large negative value of H. This characteristic is exploited by grouping clumps of contiguous negative mean curvature pixels to form image objects, and then calculating the mean of the H values for each object (Figure 4E). If a histogram is constructed from the frequency of mean H values for the objects, the silversword image objects tend to be outliers from the main peak of

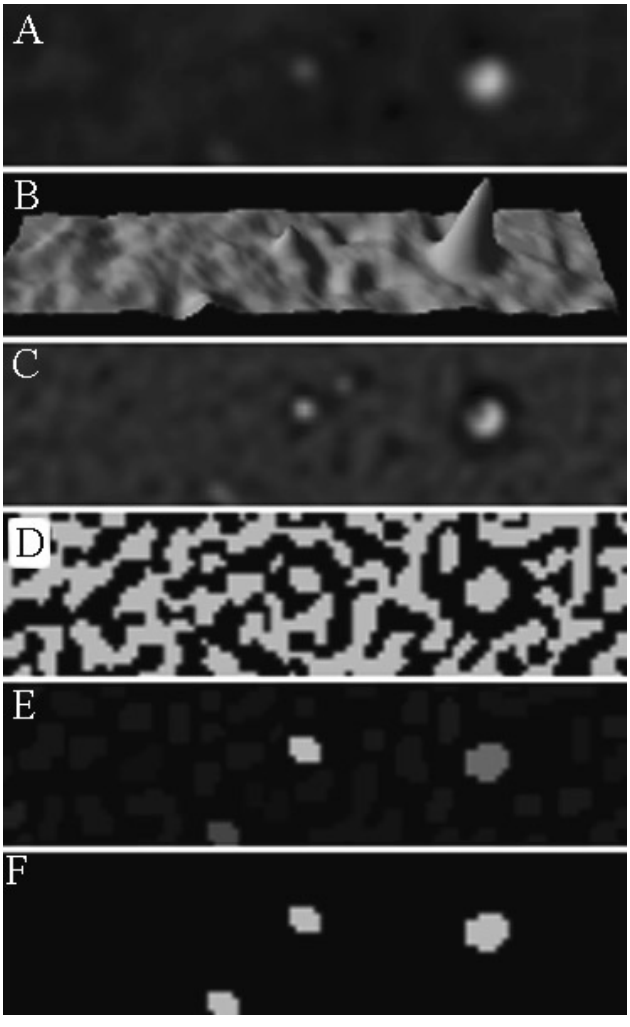

Figure 4. Diagrammatic representation of the image processing stream used in the automated census. (A) The Gaussian smoothed, normalized grey scale intensity image showing several silverswords as bright, circular objects. (B) A three-dimensional image surface, with surface height corresponding to pixel DN value. (C) Mean curvature H image representing the convex surface of several silverswords as high DN values. (D) Image showing all pixels with an H value less than zero. (E) Intensity of each connected object is then represented by its mean H value. (F) Thresholding produces a final binary image showing individual silverswords.

non-silversword objects with near-zero H values. This histogram therefore provides a useful tool for identifying a threshold of mean H that differentiates the silverswords (Figure 4F). The threshold is initially estimated through a second-order regression of the histogram (Figure 5).

In order to de-emphasize the outliers in the regression calculation, the inverse of the number of objects per histogram interval is used as a measurement error for the regression calculation. This effectively assigns a low weighting to low-frequency values in the regression.

The initial threshold is determined from the intersection of the regression line and the horizontal axis of the histogram. This automatically estimated threshold is then manually adjusted using a scaling factor, until the classification is most similar to the ground reference data. In this

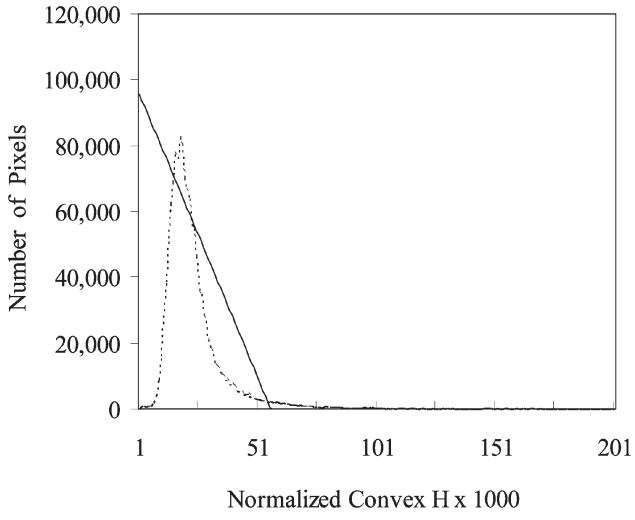

Figure 5. Distribution of normalized Convex H [--------] with second-order regression function [--------] showing threshold establishment at *x*-axis intercept.

study, a single image (census plot 7) was used to set the scaling factor for the threshold for all the remaining images. Plot 7 was selected because the rock and soil background was considered intermediate in brightness compared to the other census plots.

As an added differentiation, the relatively bright values of silversword objects were quantified using an approach similar to that of the mean H analysis. The threshold for the mean object brightness was also set using a regression-based method (Figure 6).

Only objects that meet both the mean curvature and the intensity criteria were classified as silverswords.

Silversword objects that are unusually large (we empirically chose a threshold of 25 pixels in diameter) may consist of multiple plants. The mathematical operation of opening (Russ, 1998), a procedure that separates overlapping objects, was therefore applied to large image objects. Opening is carried out as a combination of two steps. First, objects are eroded by sequentially removing the edge pix-

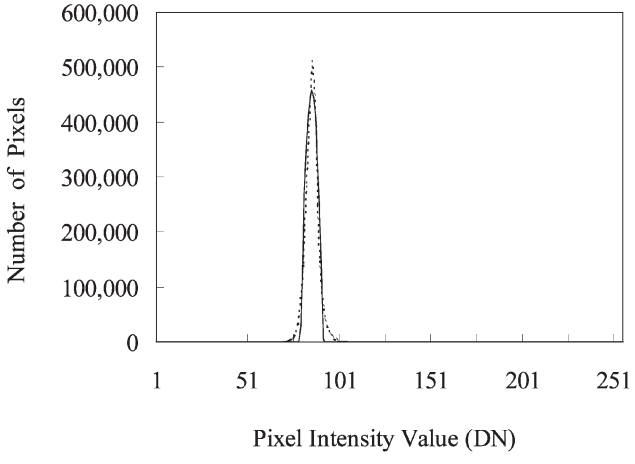

Figure 6. Pixel intensity (brightness) distribution [--------] and second-order regression function [--------] showing threshold establishment at *x*-axis intercepts.

els. This is followed by dilation, which tends to return the objects to their approximate original size, but without the complexity of the original shape. In particular, the combination of erosion and dilation tends to generalize the shapes of objects, and remove narrow protuberances. Thus, objects that are linked by narrow isthmuses should be separated into individuals by this procedure.

Human Photointerpretation Census of Silverswords

Photointerpreted images were initially processed using the custom interpolation algorithm described previously. Individual images were adjusted for contrast and brightness, and digital maps were created for each plot using the Erdas Imagine Map Composer module (Erdas, 1999). The images, measuring 8.5 by 14 inches, were printed on Kodak Inkjet photographic paper using an HP 952C color printer. Plot and subplot boundaries were printed on the images and provided a scale of reference.

For each 5- by 20-m census plot, a single 5- by 5-m subplot was randomly selected for training purposes. All training-subplot silverswords were identified, and the corresponding diameter, size class, and status (live, dead) from the 2000 field census were provided in a table. Two individuals with no previous experience with silverswords were each provided a set of nine plot images and associated training data, then asked to determine the size, size class, and status of all silverswords on the three remaining 5- by 5-m subplots on each monitoring plot. Inexperienced photointerpreters were selected because they provided a conservative estimate of aerial census accuracy. They were instructed to census each plot independently, and to record the time required for each census. Unsupervised interpretation (Nigrin, 1993), where interpreters were not provided with immediate feedback on census accuracy, was used.

Finally, monetary costs of each census method were estimated. They are provided here to assess the cost differences between the ground-based and two aerial methods, assuming that the aerial censuses were undertaken locally. Therefore, the aerial methods do not include costs of the researcher's travel and lodging. Furthermore, the time required for image processing and analysis does not include an estimate of the time required for algorithm development and testing, because these would not normally be components of an aerial silversword census for management purposes. Ground-based and aerial census costs were computed based on the U.S. Federal Government's GS-7 and GS-9 pay-scale rate of $15.00 and $20.00 (U.S.) per hour, respectively (OPM, 2000). The technicians who complete the ground-based censuses are GS-7; the GS-9 scale was used for the aerial census because of the relative technical and computational complexity required.

Accuracy Assessment

The accuracy of an aerial census of Haleakala silverswords is likely to vary as a function of silversword size and life history status. Accordingly, we evaluated census accuracy using statistical methods that considered these factors. The use of a randomly selected training plot for the human census required exclusion of one of the four subplots per plot to provide an equal comparison between photointerpretation and automated censuses, reducing the number of subplots from 36 to 27.

One-way ANOVA was used to test for differences in number of omission and commission errors per plot for the automated method and the two photointerpreters. G-tests were used to analyze the proportion of plants detected by size class for each census. Size classes were based on diameters: Class 1: seedlings (<1 cm), Class 2: 1 to 4 cm diameter, Class 3: 5 to 19 cm diameter; and Class 4: ≥20 cm diameter. Size estimation accuracy of individual silverswords was analyzed by linear regression, using the field census data as the independent variable. Logistic regression was performed on each census to describe the relationship between silversword diameter and probability of detection. The time required to complete each census was analyzed using a Kruskal-Wallis test. The analysis was limited to the time necessary to complete the census and did not consider the time required to preprocess the imagery, because this was essentially the same for aerial methods. The financial assessments are average cost per plot, and were computed by summation of the time required to accomplish each section of the image acquisition, processing, and analysis and dividing the total by the number of plots censused ($n = 9$ for aerial methods). Costs common to both aerial census methods (helicopter fees, initial image processing, input, and development of ground-reference GIS data) were assessed in full for each method, as if they were undertaken independently.

Results

Census Accuracy

Considered without respect to plant size, overall census accuracy varied by census method. For each method, accuracy was affected by error type and rate. Omission errors, where individuals were missed, are divided into "type A" and "type B." Type A omissions occurred when an individual was not detected and therefore not censused. Type B omissions occurred when two or more overlapping (clustered) silverswords were not completely segmented and were therefore counted as a single individual.

The mean number of total omissions per census plot was remarkably consistent for the automated and photointerpretation censuses ($F = 0.316$, $p = 0.73$). On average, 10.6 silverswords were omitted on each plot, equaling 38 percent of the total sample for an overall accuracy rate of 62 percent. Most omission errors were of type A, where very small silverswords were completely missed. Relatively few such errors were made by the automated procedure (Table 1). The two photointerpreters tended to overlook the same small individuals, and averaged a ten percent detection rate of plants ≤ 5 cm (9 percent and 11 percent). Photointerpreters were more effective than the automated method at detecting immediately adjacent and overlapping individuals as distinct plants, committing no type B omissions errors and having higher accuracies than the automated method in the larger size classes. The automated method made ten type B omission errors, or approximately two percent of all detections independent of size class, and 12 percent of detections in Class 3 and 4 individuals. With only three exceptions, these occurred where two or more size Class 4 individuals where growing together in a tight cluster (Figure 7).

The automated method had a significantly higher commission error rate relative to photointerpreters, misclassifying numerous unknown background objects, as well as dead rosettes, as live silverswords ($F = 13.199$, $p = 0.0001$). The

TABLE 1. CENSUS ACCURACY RATE BY SIZE CLASS FOR THE THREE AERIAL CENSUSES

Method	Size Classes 1&2 (<5 cm)*	Size Class 3 (5–19 cm)	Size Class 4 (>19 cm)
Automated	38%	73%	86%
Photointerpretation H1	9%	79%	97%
Photointerpretation H2	11%	79%	89%

* Size classes 1 and 2 have been combined and include all individuals less than 5 cm in diameter.

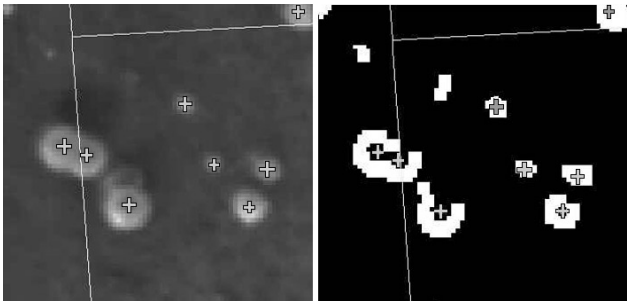

Figure 7. An example of automated errors of omission and commission. Left: grey-scale ADAR image, with plots edges superimposed and silverswords identified by grey crosses. Right: Detection of silverswords in binary image from automated method. Note the two individuals on the plot boundary have been classified as a single object, and two objects in the upper left corner have been misclassified as silverswords.

automated method averaged 25 commission errors per plot, compared to five and six for the two photointerpreters. Photointerpreters were relatively effective at differentiating bright background objects, and dead rosettes, from live silverswords, whereas the automated method identified all bright objects that exceeded the mean curvature threshold as live silverswords.

Size of individuals was an important factor in aerial census accuracy. Overall, the ability to detect individuals increased with size, although the increase depended on census method (Figure 8).

Although the automated approach was more likely to detect the smallest individuals, its advantage in the smaller sizes was not maintained across the range of diameters. Errors of omission due to incomplete segmentation of several large, clustered plants reduced detection probabilities in cases where the two interpreters effectively distinguished between them. Because of this, photointerpreters outperformed the automated method in detecting silverswords larger than 14 cm. One interpreter (Human 2) outperformed the automated method for individuals larger than 8 cm.

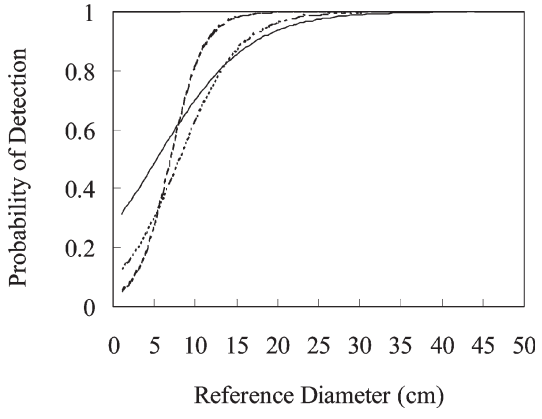

Figure 8. Logistic regression functions showing the ability to detect individual silverswords as a function of their size (diameter). The automated method [---------] had a lower type 1 omission error rate, and was more effective at detecting smaller individuals. The two photointerpreters [Human 1 -------- and Human 2 --------] had a lower type 2 omission error rate, and effectively segmented, and therefore censused, large clustered individuals.

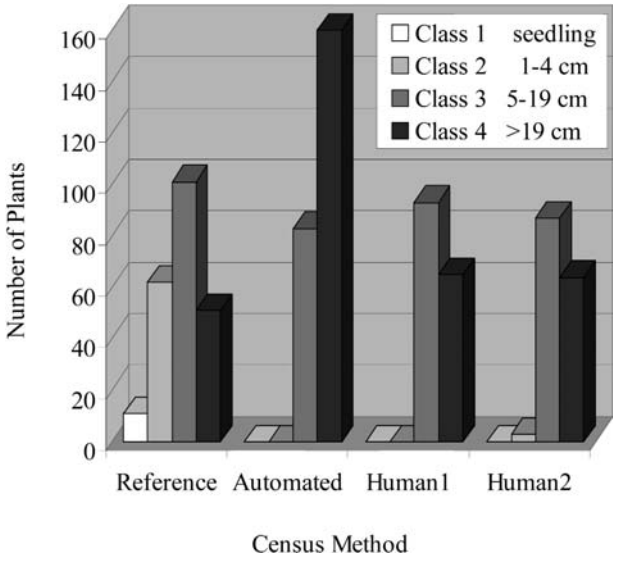

Figure 9. Number of censused individuals in each size class by census method. The reference data represent the true size class structure of the sample.

Silversword Size Class and Diameter Estimation

Although all three aerial censuses overestimated mean silversword diameter, much of the difference is explained by the missing measurements on small plants. While the reference data included many Class 1 and 2 individuals (n = 73), 90 percent of these were missed by photointerpreters and 62 percent were missed by the automated method. The size of detected plants was overestimated as well, resulting in inaccurate estimation of size class structure (Figure 9). Of the few size Class 2 individuals detected, all but three were misclassified as size Class 3. The automated method, in particular, overestimated the number of individuals in size Class 4 by consistently overestimating the diameters of Class 3 individuals.

The most accurate diameter estimates were provided by the two photointerpreters (Figure 10a, 10b, and 10c).

The ability of the automated method to accurately estimate size was limited to the largest individuals (30+ cm); the size of small (less than 10 cm), medium (10 to 19 cm), and large (20 to 30 cm) individuals was consistently overestimated. The two interpreters also overestimated the sizes of small individuals, but were generally as likely to overestimate as underestimate the diameters of medium to large individuals.

Census Time Requirements and Costs

The time required to census the plots differed significantly between the three censuses (p =0.001). One of the photointerpreters (Human 1, mean = 32.1 minutes) was significantly slower than both the other interpreter (Human 2, mean = 20 minutes; p = 0.05) and the automated method (mean = 16.6 minutes; p = 0.001). The faster of the two photointerpreters was not markedly different from the automated method. The computer processed and censused the entire image, an area about 20 times the area within an annual census plot. Assuming that silversword density on each plot was the same as density in the surrounding area,

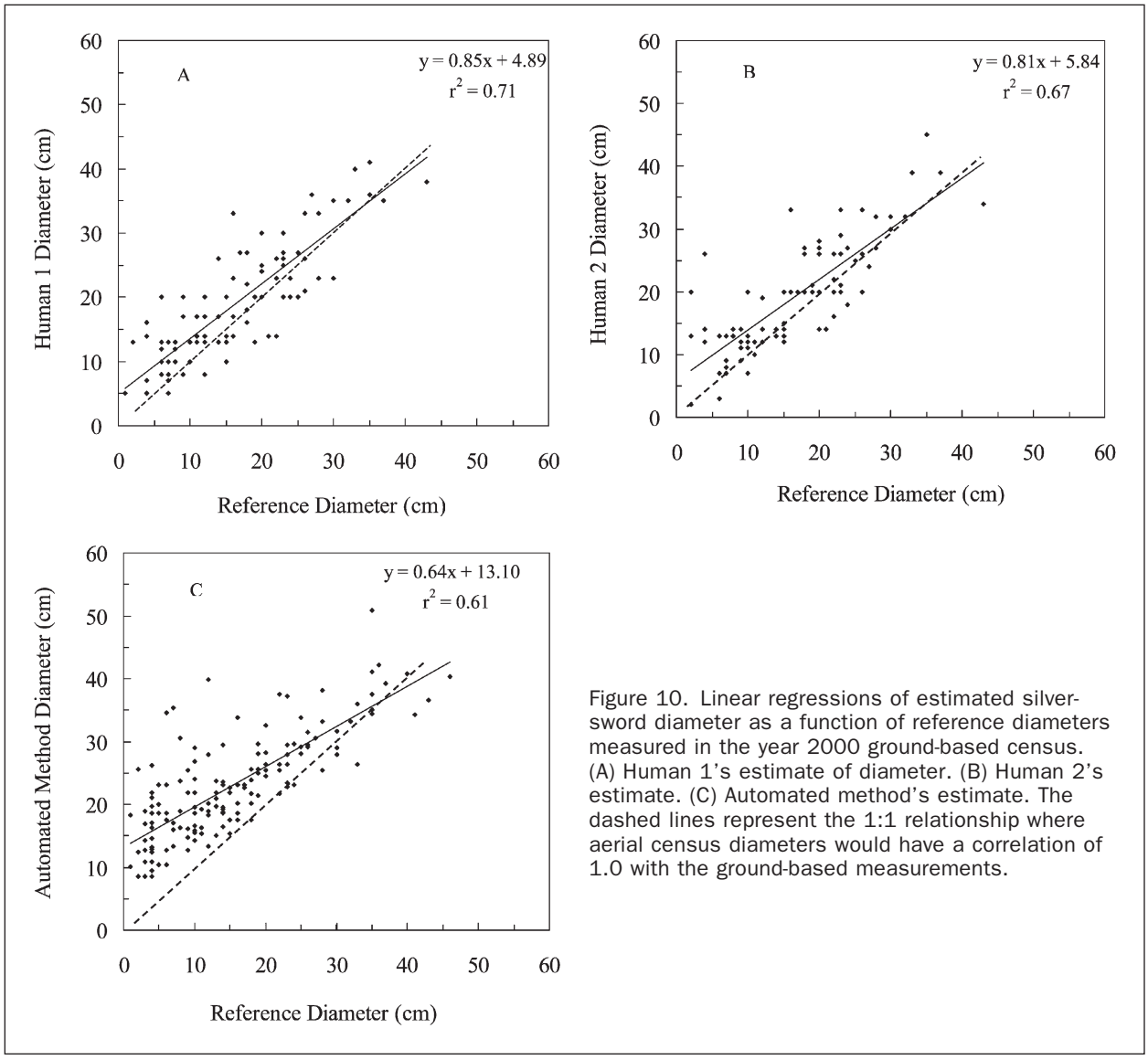

Figure 10. Linear regressions of estimated silversword diameter as a function of reference diameters measured in the year 2000 ground-based census. (A) Human 1's estimate of diameter. (B) Human 2's estimate. (C) Automated method's estimate. The dashed lines represent the 1:1 relationship where aerial census diameters would have a correlation of 1.0 with the ground-based measurements.

the computer's time to census the plot would be less than one minute. Therefore, in fact the automated method was much faster than photointerpreters on a per-plot basis.

The two aerial methods were very similar in census cost at approximately $365 per plot, while the ground-based census was substantially less expensive at approximately $110 per plot. This contrast in cost is somewhat misleading in that the aerial method with automated plant detection covered a much larger area, and more plants, than a single plot. Thus, the cost of censusing per plant may actually have been less than censusing on the ground. The per-plant cost would also be expected to decline further as more images are acquired.

The helicopter fee was the most significant component of the aerial census, and accounted for two-thirds of the total cost. Because of the time required, creation of the GIS spatial database from the scanned ground-based census maps was the second most expensive component and accounted for approximately 10 percent of the total cost. The cost of time to count silverswords in images was only 2 percent and 5 percent of the automated and photointerpretation method's associated total costs, respectively. This was approximately $7 per plot for the automated census and $20 per plot for the photointerpretation. The ground-based census was intermediate at approximately $15 per plot.

Discussion and Conclusions

This study provided a quantitative analysis of aerial census errors of omission, commission, and plant size estimation, and included an estimate of the time and costs associated with aerial censuses. Each type of census error has consequences for quantifying population dynamics and making subsequent management decisions. Type A omissions of small plants (plants that went undetected) result in underestimated recruitment rates and inaccurate estimates of size-class structure. Entire cohorts of recruited seedlings may die before they are large enough to be detected. However, because these individuals are nonreproductive, they are also least important to future population growth. One disadvantage of there being an "invisible fraction" of the population would be the existence of a lag time in detecting reduced recruitment, such as might occur with Argentine ant invasion. One potential solution to type A omission errors would be to increase image resolution. This may be achieved by using longer focal-length lenses (though scene coverage will decrease) or further technical advances with digital cameras.

Type B omissions (where an object is incompletely segmented into "true" individuals) reduce census accuracy in two potentially significant ways. First, incompletely segmented individuals, although detected, are not counted in the census; thus, the consequences are the same as with type A omissions, an underestimate of population size. Second, incomplete segmentation results in an overestimate of plant size because two or more fused plants are measured as a single plant. Type B omissions are not an issue with human photointerpreters, but further improvements are needed in the segmentation component of the automated method.

Errors of commission (where objects were incorrectly classified as live silverswords) present obvious problems for conservation monitoring due to overestimating the number of individuals. Overestimates could lead to misplaced confidence in a given population's viability. In the automated processing of visible color images, we believe these errors could be reduced by exploiting additional information about the objects, such as hue and saturation, and improving the thresholding procedure. Human photointerpreters were not restricted to using intensity data; consequently, their commission error rates were lower. This indicates that reduction of color images to DN intensity effectively reduces the type of information (hue) and the amount of information (saturation). The combined loss is significant. Finally, exploiting rear-infrared reflectance would improve distinction between live and dead plants, further reducing the number of commission errors.

Silversword diameter was quantified routinely by the automated method and manually by the two photointerpreters. Both photointerpreters and the automated method overestimated mean size; however, the size correlations of both forms of aerial censusing with ground reference data were high ($0.77 < r < 0.83$), and greater in the larger size classes. Knowing the form and magnitude of the deviation of size estimates from true sizes, one could adjust for this error in constructing size distributions. Such an adjustment presupposes the existence of ground truth plots. Therefore, where assessment of plant size matters (as it would in most plant demography applications), ground truth data will be critical.

The decision to implement a remote sensing approach to monitoring rare plants depends on several important issues, including the completeness and precision of the census data obtained (*vis-à-vis* data obtained from classical ground-based studies). However, several logistical, administrative, and ecological considerations may be equally important. For example, is the species' habitat sensitive to human presence or trampling, and conversely, are there specific environmental or social issues involving aircraft overflights? Is the habitat remote, or otherwise difficult and time consuming to access on the ground? What equipment and expertise are required for each type of census? How large a sample size can each method effectively provide? Assuming that the species is under management and aerial census and monitoring is a viable option, these questions can be addressed and resolved in the context of a species recovery plan or similar management document (Schemske *et al.*, 1994; Boersma *et al.*, 2001). Clearly, the use of aerial censuses will be most appropriate for those species whose biological and physical characteristics, habitat composition and structure, and landscape context combine to offer a data quality and logistical advantage to remote-sensing-based methods.

For federally threatened silverswords growing on remote, barren, highly erosive cinder cones in a National Park Wilderness area, aerial censuses are appropriate. Aerial methods have no physical or biological impact. Conversely, ground-based censuses require several days in the crater, and entail off-trail hiking through steep and unstable terrain, creating temporary trails and causing localized erosion. Depending on slope and substrate texture, trampling and erosion at plot locations can be substantial and could influence silversword demographics where the plants are concentrated near plot edges. Kobayashi (1973) observed "root breakage" of plants near trails, due to erosion of unconsolidated soils, resulting in rosettes tipping over under their own mass as the surrounding soils eroded.

Aerial access to crater silversword populations presents its own unique challenges. Although tourist overflights are banned because of potential impacts on wilderness values of solitude and primitive recreation, research overflight impacts can be minimized by flying in the morning before most hikers are on the floor of the crater, a time that is also more likely to yield clear skies. Alternatively, a longer focal length lens would permit imaging from higher altitudes, possibly reducing the psychological impact on wilderness visitors from low altitude overflights. Park administrators regularly use contract helicopters to service three remote visitor cabins in the Haleakala Wilderness; thus, a single annual one to two hour silversword monitoring flight per year would constitute a minimal additional impact on the wilderness experience.

Remote sensing and ground-based censuses also differ significantly in their equipment and expertise requirements. Aerial methods require a greater commitment of equipment and expertise, but also have a number of advantages. Remote sensing can gather much information over a wide geographic area in a short amount of time. Although acquisition and processing costs are much higher, the data are recorded, copied, and distributed rapidly. The spatially explicit nature of the data permits more accurate monitoring over larger geographic areas. Using image processing and GIS software, imagery can be orthorectified, co-registered, and analyzed for multiple years of data to create a multitemporal dataset. Efficient and geographically extensive spatially explicit analysis becomes possible once the data acquisition, processing, and analysis system is in place.

Aerial methods offer unique opportunities to view habitat context. Where traveling on foot immerses the individual in the local environment and allows one to focus on small-scale habitat details, aerial overflights provide a larger scale perspective where the entire landscape, including juxtaposition of habitats, ecotones, large geophysical patterns, and other features of the landscape, are observed and can be documented and analyzed in spatially explicit imagery. This information can aid in understanding the relationships between demographic patterns and processes.

The remote-sensing approach to monitoring is not necessarily a better way to census rare plant populations. Presently, there are significant censusing errors associated with the resolution limitations (for both human photointerpreters and automated object-detection routines), segmentation of individuals within the image (for the automated method), and classification of those individuals according to life history stage (for both approaches). However, this study suggests that, as the pre- and post-image processing technology improves, the advantages of remote sensing data for certain kinds of demographic studies could be significant for some applications. The large increase in extent of censuses and the spatially explicit nature of the data may open new avenues of research on population viability assessment in support of sound management decisionmaking.

Acknowledgments

The authors thank Lloyd Loope, Forrest Starr, and Kim Martz of the U.S. Geological Survey, Biological Resources

Division, Pacific Island Ecosystems Research Center for logistical support, for assistance with field work, and for providing access to the annual silversword monitoring data. The natural resources staff at Haleakala National Park expertly expedited helicopter operations and endangered species fieldwork permits. West Virginia University's Eberly College of Arts and Sciences provided funding through an ARTS grant.

References

Baldwin, B.G., D.W. Kyhos, J. Dvorak, and G.D. Carr, 1991. Chloroplast DNA evidence for a North American origin of the Hawaiian silversword alliance, *Proceedings of the National Academy of Science*, 88:1840–1843.

Bayer, B.E., 1976. *Color Imaging Array*, United States Patent 3,971,065, U.S. Patent and Trademark Office, Washington, D.C.

Beardsley, J.W., 1980. *Haleakala National Park Crater District Resources Basic Inventory: Insects*, Technical Report 31, Cooperative Park Studies Unit, Department of Botany, University of Hawaii, Honohulu, Hawaii, 68 p.

Boersma, P.D., P. Kareiva, W.F. Fagan, J.A. Clark, and J.M. Hoekstra, 2001. How good are species recovery plans? *BioScience*, 51:643–649.

Brian, M.V., 1983. *Social Insects: Ecology and Behavioral Biology*, Chapman and Hall, New York, N.Y., 377 p.

Brook, B.W., J.J. O'Grady, A.P. Chapman, M.A. Burgman, H.R. Akcakaya, and R. Frankham, 2000. Predictive accuracy of population viability analysis in conservation biology, *Nature*, 404:385–387.

Carr, G.D., 1985. Monograph of the Hawaiian Madiinae (Asteraceae): Argyroxiphium, Dubautia, and Wilkesia, *Allertonia*, 4:1–123.

———, 1987. Beggars ticks and tarweeds: Masters of adaptive radiation, *Trends in Ecology and Evolution*, 2:192–195.

Carr, G.D., E.A. Powell, and D.W. Kyhos, 1986. Self-incompatibility in the Hawaiian Madiinae (Compositae): An exception to Baker's rule, *Evolution*, 40:430–434.

Caswell, H., 2001. *Matrix Population Models*, Sinauer, Sunderland, Massachusetts, 722 p.

Cole, F.R., L.L. Loope, A.C. Madeiros, and W.W. Zuehlke, 1992. Effects of the Argentine ant on arthropod fauna of Hawaiian high-elevation shrubland, *Ecology*, 73:1313–1322.

Coultier, L., D. Stow, A. Hope, J. O'Leary, D. Turner, P. Longmire, S. Peterson, and J. Kaiser, 2000. Comparison of high spatial resolution imagery for efficient generation of GIS vegetation layers, *Photogrammetric Engineering & Remote Sensing*, 66:1329–1335.

Dean, C., T. Warner, and J. McGraw, 2000. Suitability of the DCS460C colour digital camera for quantitative remote sensing analysis of vegetation, *ISPRS Journal of Photogrammetry & Remote Sensing*, 55(2):105–118.

Erdas Inc., 1999. *Erdas Imagine Tour Guides*, *Erdas Imagine Version 8.4*, Erdas, Atlanta, Georgia, 636 p.

Gaston, K.J., 1994. *Rarity*, Population and Community Biology Series 13, Chapman and Hall, New York, N.Y., 205 p.

Gray, A., 1998. *Modern Differential Geometry of Curves and Surfaces with Mathematica*, *Second Edition*, CRC Press, Boca Raton, Florida, 1053 p.

Kobayashi, H.K., 1973. *Ecology of the Silversword,* Argyroxiphium sandwicense DC*, Haleakala Crater, Hawaii*, Ph.D. dissertation, University of Hawaii, Honolulu, Hawaii, 91 p.

———, 1991. *Status of the Haleakala silversword, Argyroxiphium sandwicense DC. ssp. macrocephalum (Gray) Meyat at Ka-Moa-o-Pele Cinder Cone and Kalahaku Overlook, Haleakala National Park*, Hawaii Natural History Association Technical Report, Maui: Haleakala National Park, 13 p.

Lloyd, R., M.E. Hodgson, and A. Stokes, 2002. Visual categorization with aerial photographs, *Annals of the Association of American Geographers*, 92(2):241–266.

Loope, L.L., and C.F. Crivellone, 1986. *Status of the Silversword in Haleakala National Park: Past and Present*, Technical Report 58, Cooperative National Park Studies Unit, Department of Botany, University of Hawaii at Manoa, Honolulu, Hawaii, 33 p.

Loope, L.L., and A.C. Madeiros, 1994. Biological invasions and rare plants in Hawaii, *Restoration of Endangered Species: Conceptual Issues, Planning, and Implementation* (M.L. Bowles and C.J. Whelan, editors), Cambridge University Press, Cambridge, United Kingdom, pp. 143–158.

McGraw, J.B., T.A. Warner, T. Key and W.R. Lamar, 1998. High spatial resolution remote sensing of forest trees, *Trends in Ecology and Evolution*, 13(8):300–301.

Menges, E.S., and D.R. Gordon, 1996. Three levels of monitoring intensity for rare plant species, *Natural Areas Journal*, 16:227-237.

Nigrin, A., 1993. *Neural Networks for Pattern Recognition*, MIT Press, Cambridge, Massachusetts, 413 p.

OPM (Office of Personnel Management), 2000. *Salary Tables for 2000*, OPM Document 124-48-6, U.S. Government Printing Office, Washington, D.C., 37 p.

Pavlik, B.M., 1994. Demographic monitoring and the recovery of endangered plants, *Restoration of Endangered Species: Conceptual Issues, Planning, and Implementation* (M.L. Bowles and C.J. Whelan, editors), Cambridge University Press, Cambridge, United Kingdom, pp. 322–350.

Perez, F.L., 2001. Geoecological alteration of surface soils by the Hawaiian silversword (*Argyroxiphium sandwicense* DC.) in Haleakala's crater, Maui, *Plant Ecology*, 157:213–231.

Peters, A.J., S.C. Griffin, A. Vina, and L. Ji, 2000. Use of remotely sensed data for assessing crop hail damage, *Photogrammetric Engineering & Remote Sensing*, 66:1349–1355.

Positive Systems Inc. 1999. *ADAR 1000 Users Manual*, Positive Systems Inc., Whitefish, Montana, 21 p.

Rade, L., and B. Westergren, 1995. *Mathematics Handbook for Science and Engineering*, Studentlitteratur, Lund, Sweden, 540 p.

Research Systems, 1999. *Using IDL*, Research Systems, Boulder, Colorado, 684 p.

Robichaux, R.H., G.D. Carr, M. Liebman, and R.W. Pearcy, 1990. Adaptive radiation of the Hawaiian silversword alliance (Compositae – Madiinae): Ecological, morphological, and physiological diversity, *Annals of the Missouri Botanical Garden*, 77:64-72.

Russ, J.C., 1998. *The Image Processing Handbook, Third Edition*, CRC Press Inc., Boca Raton, Florida, 771 p.

Schemske, D.W., B.C. Husband, M.H. Ruckelshaus, C. Goodwillie, I.M. Parker, and J.G. Bishop, 1994. Evaluating approaches to the conservation of rare and endangered plants, *Ecology*, 75:584-606.

Travis, J., and R. Sutter, 1986. Experimental designs and statistical methods for demographic studies of rare plants, *Natural Areas Journal*, 6:3-12.

Wallace, A., and S. Price, 2002. *Mean and Gaussian Curvature, CVonline: On-Line Compendium of Computer Vision* (R. Fisher, editor), URL: http://www.dai.ed.ac.uk/CVonline/LOCAL_COPIES/MARBLE/medium/surfaces/gauss.htm, last date accessed: 26 November 2002.

Wilson, E.O., and R.W. Taylor, 1967. *The Ants of Polynesia* (Hymenoptera: Formicidae), Pacific Insects Monograph 14, Bernice P. Bishop Museum Entomology Department, Honolulu, Hawaii, 96 p.

(Received 02 April 2002 April 2002; revised and accepted 30 October 2002)